Nuclear Instruments and Methods in Physics Research A 346 (1994) 550–556
North-Holland

NUCLEAR INSTRUMENTS & METHODS IN PHYSICS RESEARCH Section A

A 3-D image chamber for the liquid argon TPC based on multi-layer printed circuit board

P. Cennini [a], S. Cittolin [a], J.P. Revol [a], C. Rubbia [a], W.H. Tian [a], X. Li [b], P. Picchi [b], F. Cavanna [c], G. Piano Mortari [c], M. Verdecchia [c], D. Cline [d], Y. Liu [d], G. Muratori [d], S. Otwinowski [d], H. Wang [d], M. Zhou [d], A. Bettini [e,*], F. Casagrande [e], S. Centro [e], C. De Vecchi [e], A. Pepato [e], F. Pietropaolo [e], P. Rossi [e], S. Ventura [e], P. Benetti [f], E. Calligarich [f], R. Dolfini [f], A. Gigli Berzolari [f], F. Mauri [f], C. Montanari [f], A. Piazzoli [f], A. Rappoldi [f], U.L. Raselli [f], D. Scannicchio [f], L. Periale [g], S. Suzuki [g]

[a] *CERN, CH-1211, Geneva 23, Switzerland*
[b] *Lab. Naz. di Frascati dell'INFN, via E. Fermi 40, Frascati (Roma), Italy*
[c] *Dipartimento di Fisica e INFN, Università dell'Aquila, via Vetoio, Coppito (AQ), Italy*
[d] *Department of Physics, UCLA, Los Angeles, CA 90024, USA*
[e] *Dipartimento di Fisica e INFN, Università di Padova, via Marzolo 8, Padova, Italy*
[f] *Dipartimento di Fisica e INFN, Università di Pavia, via Bassi 6, Pavia, Italy*
[g] *ICGF del CNR di Torino, corso Fiume 4, Torino, Italy*

(Received 21 January 1994)

In our research and development programme for the ICARUS experiment we have developed a novel three-dimensional readout scheme for a liquefied noble gas TPC, where no charge multiplication process takes place. The design avoids completely wire grids and is based on the multilayer circuit technique. As a consequence it is intrinsically safe and suited to be used in large and modular structures as those foreseen for ICARUS. We describe here how the electrodes structure can be simplified leading to the new design principles and we present the results obtained with a small prototype chamber in a 100 GeV μ beam.

1. Introduction

The LAr TPC was first proposed in 1977 by Rubbia [1] with the aim to build a detector with a large sensitive mass, that is continually sensitive, self-triggering and is able to provide three-dimensional images of any ionising event, as an electronic bubble chamber. A configuration of the electrodes suitable for the three dimensional readout of the events was proposed by Gatti et al. [2]. Following these ideas we developed, in the framework of the ICARUS experiment, a multiplane wire chamber made of several parallel wire grids to be used as readout electrodes of the LAr TPC. A 3 ton prototype making use of such technology has been in operation since May 1991 [3].

The chamber works as follows. A voltage is applied to each wire plane in order to ensure the transparency of the grids to the drifting electrons (see ref. [4] for a detailed explanation of this point). The position and charge of the track elements are measured by means of the current induced on each sense wire. The drifting electrons reach and cross in sequence the following wire planes: 1) A plane of wires running in the y direction (x and y are the two orthogonal directions along which the wires are placed), functioning as a screening grid. 2) A plane of wires running again in the y direction, located below the screening grid; its function is to measure by induction the x coordinate. 3) A plane of wires running in the x direction located below the previous plane; its function is to measure the y coordinate. Since this is the last sensitive plane, the electric field is such that this plane collects the drifting electrons.

An electron drifting in the sensitive volume above the screening grid does not produce any current in the coordinate planes (in the case of perfect shielding). A positive induced current starts in the x coordinate plane when the electron crosses the screening grid, becomes negative when the electron crosses the coordinate plane and ends when the electron crosses the y coordinate plane. The charge

* Corresponding author. Tel. +39 49 844 207, fax +39 49 844 245.

0168-9002/94/$07.00 © 1994 – Elsevier Science B.V. All rights reserved
SSDI 0168-9002(94)00164-3

signal from the y coordinate plane has similar behaviour, with the exception that only the positive current is present.

The originality and the performance of this technique, that we will call "wire R/O" in the following, applied to wire chambers of dimension up to 2.5 m^2 and of 2 mm grid pitch, have been discussed in detail in a recent paper [5]. Continuing our research and development program, we have searched for an alternative technique to read out the charge of the ionisation electrons, avoiding the use of any wire plane. The aim of this paper is to present a new technique, based on printed circuit boards ("PCB R/O"), that is suitable for building large size 3-D image chambers with an intrinsically safe structure and performance comparable to that of the wire chamber technique.

In our experience with the wire R/O we have found that the performance and the reliability of the system should be improved, specifically in the following aspects.

Mechanics: The wire chamber R/O makes use of a large number of wires, that must be kept in place, without bending. This implies accurate positioning (combs), high stress (several kilograms) and very robust and thick frames. A possible loosening of one wire, due for example to thermal stress, can make an appreciable part of the detector unusable.

Electronics: large electric fields (of the order of several kV/cm) are necessary to ensure the correct path of the drifting electrons through the grids without unwanted losses. This implies increased stress to the wires due to electrostatic forces and the necessity of high voltage decoupling capacitors.

Analaysis: The induction signals are fast (both rise and fall times are a few microseconds long), resulting in few points on the sampled output; this decreases the efficiency of the filtering algorithms needed to enhance the signal to noise ratio. For the same reason we can extract from the induction signals only the arrival time. The charge (pulse height) and rise time are extracted from the collection signals.

2. The new image chamber

To understand the new structure of the image chamber let us start from the following configuration of the wire planes readout electrodes:

1) a screening grid, made of parallel wires (100 μm in diameter) with a 3 mm pitch (line of open circles in Fig. 1a);

2) a collection plane, located 3 mm below the screen, also made of parallel wires (100 μm in diameter) and oriented in the same direction as those of the grid; their functions are alternatively of field shaping wires (open circles in Fig. 1a) and of sense wires (full circles), where the drifting electrons are collected; the distance between two collection wires is 3 mm (continuous line);

3) a conductive plane at a distance of 0.5 mm.

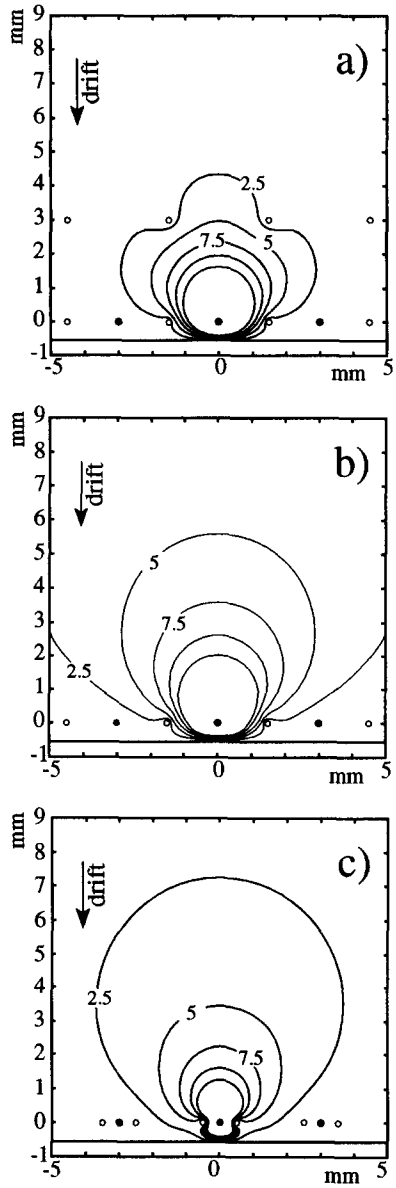

Fig. 1. Equi-induction curves for the collection electrodes in the plane normal to the collection electrodes and parallel to the drift field for the three structures described in the text. (a) Wire chamber with screen grid. (b) Chamber without screen grid. (c) Chamber without grid with a different electrodes configuration.

Fig. 1a shows the map of the equi-induction contours calculated for the structure described above; the shape of these lines depends only on the geometry of the electrodes. A point charge placed anywhere in the space induces a fraction of its charge on the electrode (sense wire) under

examination (the wire at 0,0 co-ordinates in Fig. 1a) equal to the value of the contour line passing through the charge position (the percentage of induced charge is used to label the curves). Equi-induction lines become very close one to the other near the wire. For this reason lines with induction above 12.5% have not been drawn. As desired, the induction is appreciable only close to the wire; the screening grid helps by "pushing" the line below its plane: this is in fact its shielding contribution.

We now proceed to simplify the electrode structure. The first step consists in eliminating the screening grid. The equi-induction curves are presented in Fig. 1b (open circles are screen wires, full circles are sense wires). A comparison with the previous configuration shows that, as expected, the lines corresponding to the same induction now spread further away in the drift space. Notice that, on the other hand, the residual but effective shielding function is now performed by the screening wires that are co-planar with the sense wires and by the conductive plane.

The shielding action can be improved by positioning the screening wires closer to the sense wires. We consider a configuration with two screening wires on each side of a sense wire and at a distance of 0.5 mm. The calculated equi-induction map is shown in Fig. 1c (open circles are screen wires, full circles are sense wires). In this new configuration the curves are nearer to the sense wires, similar to those of Fig. 1a, for which the grid was present.

We next discuss how to use the "non-gridded" configuration for a 3-D imaging readout. The wire plane represented in Fig. 1b or 1c can be used as the collection plane by giving a suitable potential difference between field and sense wires, to focus the field lines on the collection wires. In practice we polarize the sense wires at +300 V and the field wires at −300 V, in order to keep the average potential of the collection plane at ground. To measure the second coordinate we must have an induction electrode plane.

In the wire configuration the induction plane was placed in front of the collection plane and the voltage applied was such that the induction plane was completely transparent to the drifting electrons. In this scheme the drifting electrons, moving across this plane, give by induction the signal to be detected; they then move toward the second plane where they are collected. In the new configuration we substitute the conductive plane behind the collection grid with a plane made of parallel electrodes acting as the induction plane. In fact the induction signal due to electrons moving above the collection plane is visible even below the collection plane because the latter does not act as a perfect screen. The problem is to try to maximise this induction signal without deteriorating the collection signal. The simplest way consists in increasing the width of the induction electrodes while minimising that of the collection electrodes, in order to favour the charge induced on the induction plane due to the solid angle effect, and in working with a small gap between the two planes.

The equi-induction map for the induction electrodes is shown in Fig. 2b for a configuration consisting of a collection plane as that of Fig. 1b and of an induction plane located 0.5 mm below it made of sense strips 2.54 mm wide with a 3 mm pitch. The map is in a plane parallel to the field and at 45° with induction and collection electrodes. It refers to the electrode in the centre of the figure.

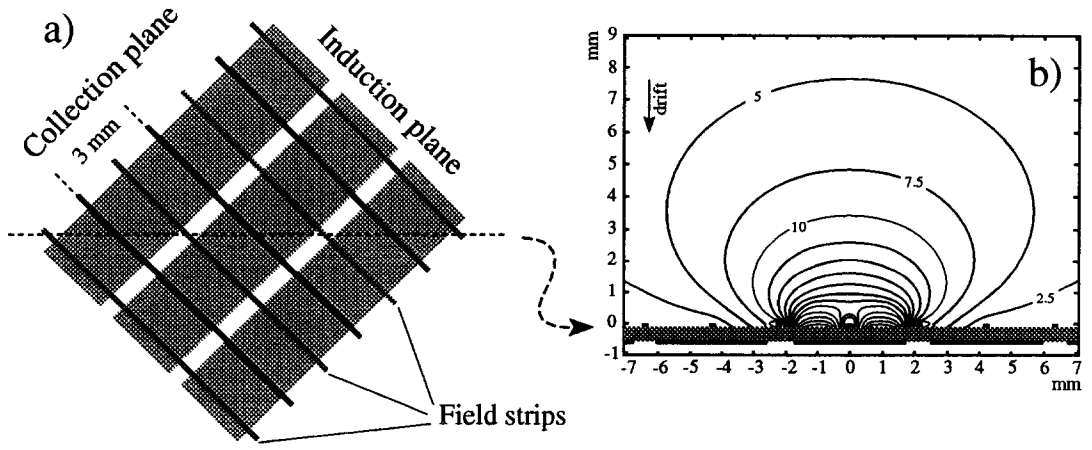

Fig. 2. (a) Schematics of the collection and induction planes. (b) Resulting equi-induction curves in a plane perpendicular to the collection and induction planes at 45° with both collection and induction electrodes.

We are now ready for the second and last step in the simplification process. A very important feature of the new configuration is that the drifting electrons never cross any grid. As a consequence, the structure can be made of metal strips deposited on the two faces of a dielectric support employing, in practice, printed circuit techniques.

We have constructed a readout structure consisting of a 0.5 mm thick vetronite sheet with the collection strips on the upper face and the induction strips on the lower one. The rigidity of the structure is obtained with a second vetronite sheet, 2 mm thick, glued on the lower side. Collection and induction strips are mutually perpendicular and have both a 3 mm pitch. The collection strips are 0.1 mm wide, while the induction ones are 2.54 mm wide. Two field strips (0.1 mm wide) are located at the two sides of each collection strip, on the same plane and at distance of 0.5 mm.

We now compare the collection and induction signal shapes in the configurations of Fig. 1a (gridded) and of Fig. 1b (ungridded). First we calculate the time dependence of the signal induced on the sense wire by moving the charge of a track segment along trajectories parallel to the drift field with appropriate velocities. We will consider tracks parallel to the readout planes. Fig. 3a shows the result of our calculation for the "gridded" configuration of Fig. 1a. For comparison we also show, superimposed, an experimental signal collected with a small LAr TPC exposed to a μ beam (see section 3). The excellent agreement denotes the reliability of our calculation.

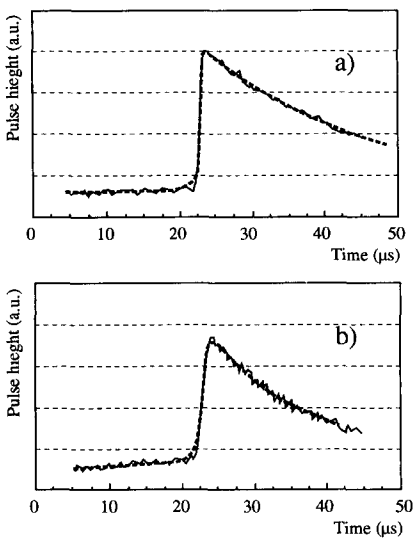

Fig. 3. Measured and calculated shapes for the "collection" signals for (a) the gridded configuration and (b) the ungridded configuration. Pulse heights are in arbitrary units.

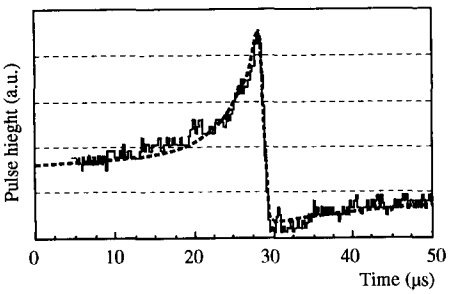

Fig. 4. Measured and calculated shapes for the "induction" signal for the ugridded configuration. Pulse heights are in arbitrary units.

The signal shape (theoretical and experimental) for the "ungridded" configuration of Fig. 1b is shown in Fig. 3b; the main difference with the shape of Fig. 3a is in the long leading tail which is due to the shielding inefficiency (it appears as a slowly increasing base line). Nevertheless the main physical parameters (pulse height, arrival time, signal slope) can be extracted with equal reliability from the collection signal shapes in both configurations described above.

The calculated induction signal shape, superimposed on a real pulse, for the ungridded configuration of Fig. 1b, is shown in Fig. 4. Note that the induction signal now has a shape, and height, very similar to that of the collection one (but of opposite polarity); this could lead to a more reliable extraction of the physical parameters also for the induction case.

We stress here that, from a practical point of view, a very important feature of this new configuration is that a chamber can be constructed on a printed circuit board. The fact of having eliminated all the wires makes the structure intrinsically safer and stable. Another advantage is that the voltage difference applied on the collection electrodes is now very small (a few hundreds of volts); this leads to a more uniform electric field in the drift volume and the use of smaller and safer decoupling capacitors. As a consequence the front-end electronics can be located very close to the chamber, even inside the LAr, thus avoiding long cables that increase the input capacitance (and hence the series noise) and the microphonic pick-up. In addition, as a by-product, the connections of the sense electrodes to the front-end electronics and the high-voltage distribution can be realised as an integrated part of this printed circuit board (making use of the multilayer technique).

A possible drawback of this solution is the increase of the detector capacitance due to two factors: the reduction of the inter-plane gap (in our case from 3 mm to 0.5 mm) and the higher dielectric constant of the printed circuit support with respect to that of argon ($\epsilon_r = 1.5$). This could worsen the S/N ratio and therefore degrade the detector performance. A way to partially avoid this problem con-

sists in using a support with low dielectric constant (e.g. Teflon, $\epsilon_r = 2.2$) and to divide each strip into segments of the order of a few metres, each of which is read by one preamplifier whose output is then "ORed" with that of the other segments. A realistic value of the achievable specific capacitance is about 20–30 pF/m, not different from that of the wire chamber.

3. Experimental results

To compare with real data the performance of the two configurations described in the previous sections, we built two small 3-D image chambers, one using the wire technique, the other the printed board technique. The wire chamber consisted of a sequence of three wire planes: the grid (100 μm diameter wires with 3 mm pitch), the induction plane (100 μm diameter wires with 3 mm pitch, sense and field wires interleaved), the collection plane (same geometry as the induction plane, with wires perpendicular to the induction wires). The distance between two contiguous planes was 3 mm. The second chamber had the configuration shown in Fig. 1b and Fig. 2. The number of sense wires was 19 in both induction and collection cases. These chambers were used in turn as readout electrodes of a LAr TPC whose drift length was 13 cm. We exposed the TPC to the CERN-SPS 100 GeV μ beam.

The TPC was placed with the drift electric field parallel to the floor and with the possibility of rotating it around a vertical axis (see Fig. 5a). The wire chamber was placed with the collection wires vertical, in order to see the signal due to the ionising beam on all the collection wires. Since the induction electrodes are horizontal, only one of them was hit in each event.

In the printed board case, instead, a rotation of 36° around the drift axis was given to the board in such a way that a track image, made of several contiguous wire hits, was visible on both the collection and induction planes; the image of a multitrack event can be seen in Fig. 6. We measured the detector response to minimum ionising particles (m.i.p.), in terms of energy and spatial resolution, as a function of the electric field strength and of the angle between the track and the drift direction.

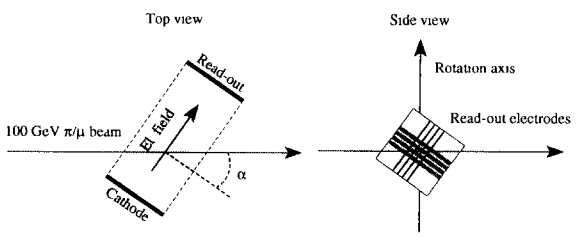

Fig. 5. Schematics of the TPC layout in the beam. In the right part the field is perpendicular to the paper.

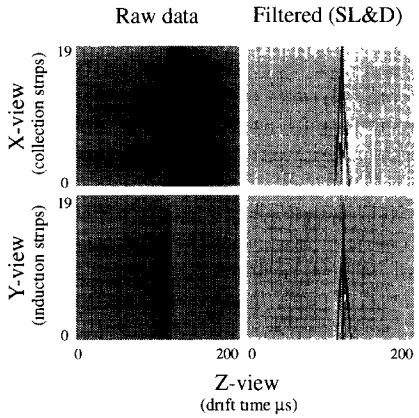

Fig. 6. The two orthogonal views (raw and filtered data, the filter uses a slide and difference technique) of a three-prong interaction from the multilayer chamber.

3.1. Electron lifetime

A first important result is that no appreciable difference in the electron lifetime has been observed over a period of more than a month (it was always higher than 3 ms) in the two cases. This confirms [6] that at LAr temperature the outgassing of electronegative impurities from any material employed in the construction of the TPC is negligible.

3.2. Energy resolution

The energy resolution can be extracted from the distribution of the charge deposited by minimum ionising particles on single sense strips by fitting the distribution with the convolution of Landau and Gaussian functions. This is possible because the relation between the energy deposited and the charge collected dominated by the electron–ion recombination for minimum ionising particles, is linear around the Landau peak. The Landau parameter is related to the intrinsic fluctuation of dE/dx in LAr, while the variance of the Gaussian takes into account the contribution of the electronic noise, calibration and the signal extraction algorithm.

The results obtained with both readout chambers are very similar: the Landau parameter is around 800 electrons, in agreement with the value predicted by the Vavilov model [7]; the overall Gaussian noise is about 400 electrons in agreement with the measurement done on the width of the test pulse height distribution. In Fig. 7 we present the two distributions of the charge deposited on the collection electrodes obtained with the multilayer chamber and with the wire chamber. The data correspond to tracks

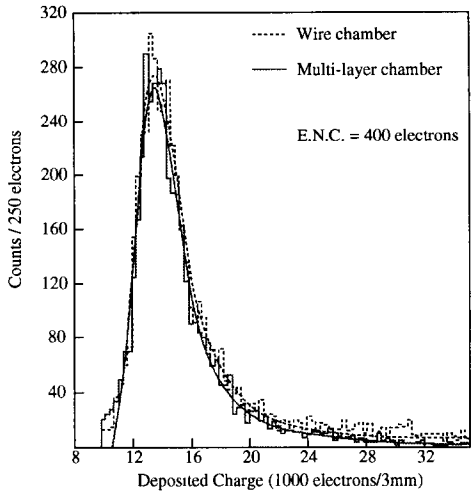

Fig. 7. Collected charge distributions on 3 mm track length for beam particles crossing the chamber parallel to the electrode plane for both the wire chamber and the multilayer chamber.

running parallel to the chamber plane and to a drift field of 500 V/cm. The good agreement is evident.

3.3. Electric field and angular dependence of the free electron yield

The peak in the charge distributions can be used to measure the electric field dependence of the charge released by a m.i.p. over 3 mm and, as a consequence, the electron–ion recombination effect. Moreover the data taken with the beam can be used to measure the dependence of the collected charge on the angle (α in Fig. 5) between the electric field lines and the track direction. Angle dependent effects could be induced by the absence of a screening grid in the multilayer chamber. Such a dependence could worsen the overall energy resolution mainly for low energy tracks (e.g.: few MeV electrons) for which multiple scattering makes the track direction vary considerably even within a single wire pitch.

The experimental data are presented in Fig. 8: the peak of charge distribution at each angle normalised to the wire pitch (3 mm) is plotted against the track angle for two electric field strengths (500 V/cm and 1 kV/cm) for both readout chambers. The slight increase visible at large angles is due to the change of the effective track sampling pitch (3 mm at 0°, 6 mm at 60° and 9 mm at 70°) which in turn introduces a well known peak shift in the normalised Landau distribution. This is confirmed by the analysis performed on Monte Carlo data. The agreement between the two chambers is fully satisfactory both for the electric field dependence and the angular behaviour.

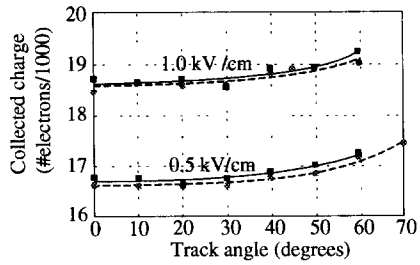

Fig. 8. Angular dependence of the (peak position) collected charge for both the wire chamber (grey dots and dotted lines) and the multilayer chamber (black squares and continuous line) at two different drift fields.

3.4. Spatial resolution

The single point space resolution along the drift direction can be evaluated by a linear fit event by event of the arrival times versus the wire positions with a straight line and by extracting the distribution of the residuals to the fit. The width of the distribution gives the arrival time resolution. The best result is obtained if the straight line fit is made, using three contiguous wires at the time, to minimise the contribution from multiple scattering. Knowing the electron drift velocity it is straightforward to obtain the single point space resolution. In Fig. 9 we show both the resolution on the drift time measurement and the space resolution (obtained from the latter multiplying by the drift velocity) versus the electric field. Time resolution worsen at lower fields due to the diffusion of the charge drifting for longer times; on the other hand, space resolution becomes better because the decrease of the drift velocity overcompensates the effect of the broadening of the signal. For the present discussion it is important to notice that for both readout chambers no appreciable difference was measured.

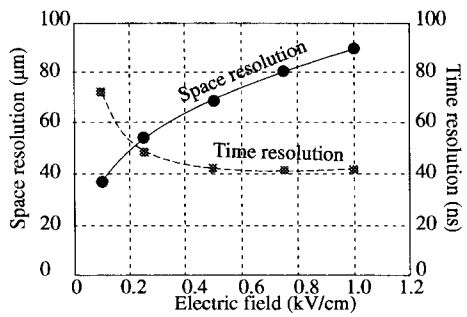

Fig. 9. Resolution in the drift time measurement (right scale) and space resolution in the drift coordinate measurement (left scale) as functions of the drift field.

4. Conclusion

We have developed a new 3-D imaging read-out structure suitable to be employed in any liquefied noble gas TPC where no charge multiplication process occurs. The design, based on the multi-layer printed circuit board technique, is intrinsically safe, both mechanically and electrically. Large size and modular structures are foreseen for the ICARUS experiment at Gran Sasso [8]. An encouraging step forward has been achieved in increasing the reliability of the technique, but further research and development work is needed, building a full size prototype, before reaching a final conclusion. In addition the printed board R/O scheme allows to vary the pitch of the segmented electrodes within the same detector. This feature is particularly appropriate for the ICARUS experiment because it enhances its intrinsic characteristic of being a multipurpose device.

References

[1] C. Rubbia, CERN-EP Internal Report 77-8 (1977).
[2] E. Gatti et al., IEEE Trans. Nucl. Sci. NS-26 (1979) 2910.
[3] P. Benetti et al., Nucl. Instr. and Meth. A 322 (1993) 395.
[4] O. Bunemann et al. Can. J. Res. 27 (1947) 191.
[5] P. Benetti et al., submitted to Nucl. Instr. and Meth.
[6] A. Bettini et al., Nucl. Instr. and Meth. A 305 (1991) 177.
[7] P.V. Vavilov, Sov. Phys. JETP 5 (1957) 749.
[8] ICARUS Collaboration, ICARUS II, a second generation proton decay experiment and neutrino observatory at the Gran Sasso Laboratory, proposal vol. I, 22 September 1993.